

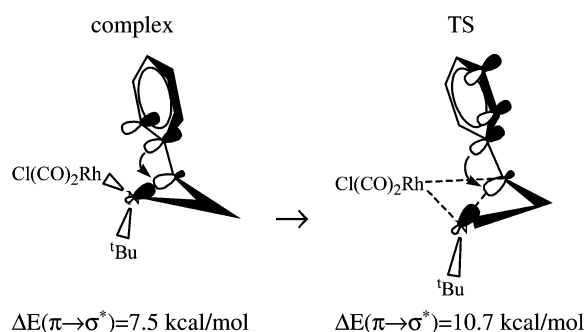
# A Theoretical Study of Rhodium(I) Catalyzed Carbonylative Ring Expansion of Aziridines to $\beta$ -Lactams: Crucial Activation of the Breaking C–N Bond by Hyperconjugation

Diego Ardura, Ramón López, and Tomás L. Sordo\*

Departamento de Química Física y Analítica, Universidad de Oviedo,  
Julián Clavería, 8, E-33006 Oviedo, Spain

tsordo@uniovi.es

Received May 22, 2006



The regioselectivity and enantiospecificity of the  $[\text{Rh}(\text{CO})_2\text{Cl}]_2$ -catalyzed carbonylative ring expansions of *N*-*tert*-butyl-2-phenylaziridine to yield 2-azetidinone and the lack of reactivity of *N*-*tert*-butyl-2-methylaziridine along this process were investigated at the B3LYP/6-31G(d) (LANL2DZ for Rh) theory level taking into account solvent effects. According to our results, the regioselectivity in the ring expansion of *N*-*tert*-butyl-2-phenylaziridine and the unreactivity of *N*-*tert*-butyl-2-methylaziridine experimentally observed are determined by the different degree of activation of the breaking C–N bond in the initial aziridine- $\text{Rh}(\text{CO})_2\text{Cl}$  complex due to its hyperconjugation interaction with the substituent on the carbon atom. When a phenyl substituent is present its hyperconjugation interaction with the  $\text{C}_\alpha$ –N bond facilitates the insertion of the metal atom into this bond. On the other hand, when the substituent is a methyl group, a larger stability of the initial complex along with a lower stabilization through hyperconjugation of the TS for insertion of the Rh atom into the  $\text{C}_\alpha$ –N bond make the ring expansion of *N*-*tert*-butyl-2-methylaziridine unviable. The enantiospecificity experimentally observed is also reproduced by our calculations given that the stereogenic center is never perturbed to change its configuration.

## Introduction

Since the elucidation of the structure of penicillin by Crowfoot-Hodgkin et al. in 1945,<sup>1</sup>  $\beta$ -lactams have become the center of attention for many synthetic, medicinal, and theoretical chemists and biologists because of their utility as synthetic intermediates and their biological activity.<sup>2–11</sup> As a consequence,

a large number of chemical methods for the production of  $\beta$ -lactams have been proposed.<sup>8,9</sup> One of these synthetic strategies is the carbonylative ring expansion of aziridines

\* To whom correspondence should be addressed. Tel: +34 98 5 103 475. Fax: +34 98 5 103 1255.

(1) Crowfoot, D.; Bunn, C. W.; Rogers-Low, B. W.; Turner-Jones, A. In *The Chemistry of Penicillin*; Clarke, H. T., Johnson, J. R., Robinson, R., Eds.; Princeton University Press: Princeton, NJ, 1949; Chapter 11, p 310.

(2) *Chemistry and Biology of  $\beta$ -Lactam Antibiotics*, Morin, R. B., Gorman, M., Eds.; Academic Press: New York, 1982; Vols. 1–3.

(3) Dürkheimer, W.; Blumbach, J.; Lattrell, R.; Scheunemann, K. H. *Ang. Chem., Int. Ed. Engl.* **1985**, *24*, 180.

(4) *The Chemistry of  $\beta$ -Lactams*; Page, M. I., Ed.; Blackie Academic & Professional: London, 1992.

(5) *The Organic Chemistry of  $\beta$ -Lactams*; Georg, G. I., Ed.; VCH: Weinheim, 1992.

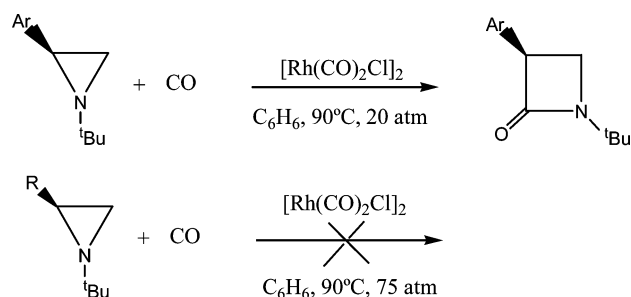
(6) Southgate, R. *Contemp. Org. Synth.* **1994**, *1*, 417.

(7) Nicolau, K. C.; Sorensen, E. J. *Classics in Total Synthesis*, VCH: Weinheim, 1996.

(8) López, R.; del Río, E.; Díaz, N.; Suárez, D.; Menéndez, M. I.; Sordo, T. L. *Recent Res. Dev. Phys. Chem.* **1998**, *2*, 245.

(9) Palomo, C.; Aizpurua, J. M.; Ganboa, I.; Oiarbide, M. *Eur. J. Org. Chem.* **1999**, 3223.

## SCHEME 1



catalyzed by metallic complexes,<sup>12–27</sup> which presents an intriguing regio-, stereo-, and enantioselectivity depending on the nature of the metal catalyst and the substituents on the ring atoms.

One of the pioneering works on these kinds of processes has been the rhodium-catalyzed carbonylative ring expansion of aziridines,<sup>12</sup> which has proved to be a versatile reaction for the regioselective, stereospecific, and enantiospecific synthesis of  $\beta$ -lactams in excellent yields.<sup>15</sup> The interest in the  $[\text{Rh}(\text{CO})_2\text{Cl}]_2$ -catalyzed carbonylative ring expansion of aziridines has recently been renewed owing to the use of rhodium-complexed dendrimers on a resin as catalysts.<sup>27</sup> Many aziridines can be employed in this reaction, but the presence of an aryl group  $\alpha$  to N is essential.<sup>19</sup> It has been suggested<sup>15</sup> that the arene ring of the aziridine initially coordinates to the Rh(I) complex, facilitating insertion of the metal atom into the more substituted of the two C–N bonds to give a Rh(III) complex. Subsequent insertion of a CO ligand into the N–Rh bond would form a five-membered ring structure in a regioselective way. Carbonylation of this structure on the Rh atom followed by a reductive elimination would render the final  $\beta$ -lactam.<sup>15</sup> These processes proceed with retention of the configuration of the  $\alpha$  carbon atom. The carbonylative ring expansion of 2-aryl aziridines gives 3-aryl-2-azetidinones in 97–100% yields depending on the substituents on the  $\alpha$  carbon atom, whereas 2-alkylaziridines are recovered unchanged (see Scheme 1). In this paper we present the first theoretical study of the mechanism for the  $[\text{Rh}(\text{CO})_2\text{Cl}]_2$ -catalyzed carbonylative ring expansion of *N*-*tert*-butyl-2-phenylaziridine to form the  $\beta$ -lactam ring, focusing our attention on the regioselectivity and the enantiospecificity of

the process. We also investigated the  $[\text{Rh}(\text{CO})_2\text{Cl}]_2$ -catalyzed carbonylative ring expansion of *N*-*tert*-butyl-2-methylaziridine to yield the corresponding 2-azetidinone, which has been experimentally found not to take place, trying to understand this behavior.

## Computational Methods

Quantum chemical computations were carried out with the Gaussian 98 series of programs<sup>28</sup> employing the hybrid density functional B3LYP,<sup>29–31</sup> which combines Becke's three-parameter nonlocal hybrid exchange potential with the nonlocal correlation functional of Lee, Yang, and Parr. Full geometry optimizations of stable species and transition states (TS) were performed in the gas phase by using the LANL2DZ effective core potential for Rh<sup>32,33</sup> and the 6-31G(d) basis set<sup>34</sup> for the remaining atoms through the standard Schlegel's algorithm.<sup>35</sup> The nature of the stationary points was verified by analytical computations of harmonic vibrational frequencies. This theory level has proved adequate to the study of  $[\text{Rh}(\text{CO})_2\text{Cl}]_2$ -catalyzed intermolecular [5 + 2] reactions between vinylcyclopropanes and alkynes.<sup>36</sup> Intrinsic reaction coordinate (IRC) calculations with the Gonzalez and Schlegel method have been used to check the two minimum energy structures connecting each TS.<sup>37,38</sup>

To take into account condensed-phase effects, we evaluated the energy in solution of all the species using the polarizable continuum model (PCM)<sup>39,40</sup> of Tomasi et al. with the united atom Hartree–Fock (UAHF) parametrization.<sup>41</sup> This energy in solution comprises the electronic energy of the polarized solute, the electrostatic solute–solvent interaction energy  $\langle \Psi_i | \mathbf{H} + 1/2 \mathbf{V}_i | \Psi_i \rangle$ , and the non-electrostatic terms corresponding to cavitation, dispersion, and short range repulsion. A relative permittivity of 2.247 was assumed in the calculations to simulate benzene as the solvent experimentally used.

A natural bond orbital (NBO) analysis was performed on the most important critical structures located along the reaction coordinates.<sup>42,43</sup>

## Computational Results

We will present first the results corresponding to the  $[\text{Rh}(\text{CO})_2\text{Cl}]_2$ -catalyzed ring expansion of (*S*)-*N*-*tert*-butyl-2-phenylaziridine and then those corresponding to (*S*)-*N*-*tert*-butyl-2-methylaziridine. In Figure 1 and Tables 1S, 3S, and 5S in Supporting Information we present the results for the attack of  $\text{Rh}(\text{CO})_2\text{Cl}$  on the C–N bond bearing the phenyl or methyl substituents. Figure 2 and Tables 2S and 4S in Supporting Information display the data corresponding to the attack of  $\text{Rh}(\text{CO})_2\text{Cl}$  on the nonsubstituted C–N bond of (*S*)-*N*-*tert*-butyl-

(10) López, R.; Menéndez, M. I.; Díaz, N.; Suárez, D.; Campomanes, P.; Sordo, T. L. *Recent Res. Dev. Phys. Chem.* **2000**, *4*, 157.

(11) López, R.; Menéndez, M. I.; Díaz, N.; Suárez, D.; Campomanes, P.; Ardura, D.; Sordo, T. L. *Curr. Org. Chem.* **2006**, *10*, 805.

(12) Alper, H.; Urso, F.; Smith, D. J. H. *J. Am. Chem. Soc.* **1983**, *105*, 6737.

(13) Alper, H.; Hamel, H. *Tetrahedron Lett.* **1987**, 3237.

(14) Chamchaang, W.; Pinhas, A. R. *J. Chem. Soc., Chem. Commun.* **1988**, 710.

(15) Calet, S.; Urso, F.; Alper, H. *J. Am. Chem. Soc.* **1989**, *111*, 931.

(16) Chamchaang, W.; Pinhas, A. R. *J. Org. Chem.* **1990**, *55*, 2943.

(17) Spears, G. W.; Nakanishi, K.; Ohfuné, Y. *Synlett* **1991**, 91.

(18) Tanner, D.; Somfai, P. *Bioorg. Med. Chem. Lett.* **1993**, *3*, 2415.

(19) Khumtaveeporn, K.; Alper, H. *Acc. Chem. Res.* **1995**, *28*, 414.

(20) Piotti, M. E.; Alper, H. *J. Am. Chem. Soc.* **1996**, *118*, 111.

(21) Ley, S. V.; Middleton, B. *Chem. Commun.* **1998**, 1995.

(22) Davoli, P.; Moretti, I.; Prati, F.; Alper, H. *J. Org. Chem.* **1999**, *64*, 518.

(23) Davoli, P.; Prati, F. *Heterocycles* **2000**, *53*, 2379.

(24) Davoli, P.; Forni, A.; Moretti, I.; Prati, F.; Torre, G. *Tetrahedron* **2001**, *57*, 1801.

(25) Lee, J. T.; Thomas, P. J.; Alper, H. *J. Org. Chem.* **2001**, *66*, 5424.

(26) Mahadevan, V.; Getzler, Y. D. Y. L.; Coates, G. W. *Angew. Chem., Int. Ed.* **2002**, *41*, 2781.

(27) Lu, S. M.; Alper, H. *J. Org. Chem.* **2004**, *69*, 3558.

(28) Frisch, M. J. et al. *Gaussian 98*, Revision A.6; Gaussian, Inc., Pittsburgh, PA, 1998.

(29) Becke, A. D. *Phys. Rev. A* **1988**, *38*, 3098.

(30) Lee, C.; Yang, W.; Parr, R. G. *Phys. Rev. B* **1988**, *37*, 785.

(31) Becke, A. D. *J. Chem. Phys.* **1993**, *98*, 5648.

(32) Hay, P. J.; Wadt, W. R. *J. Chem. Phys.* **1985**, *82*, 299.

(33) Wadt, W. R.; Hay, P. J. *J. Chem. Phys.* **1985**, *82*, 284.

(34) Hehre, W. J.; Radom, L.; Pople, J. A.; Schleyer, P. v. R. *Ab Initio Molecular Orbital Theory*; Wiley: New York, 1986.

(35) Schlegel, H. B. *J. Comput. Chem.* **1982**, *3*, 214.

(36) Yu, Z. X.; Wender, P. A.; Houk, K. N. *J. Am. Chem. Soc.* **2004**, *126*, 9154.

(37) Gonzalez, C.; Schlegel, H. B. *J. Phys. Chem.* **1989**, *90*, 2154.

(38) Gonzalez, C.; Schlegel, H. B. *J. Phys. Chem.* **1990**, *94*, 5523.

(39) Tomasi, J.; Persico, M. *Chem. Rev.* **1994**, *94*, 2027.

(40) Tomasi, J.; Cammi, R. *J. Comput. Chem.* **1995**, *16*, 1449.

(41) Barone, V.; Cossi, M.; Tomasi, J. *J. Chem. Phys.* **1997**, *107*, 3210.

(42) Reed, E.; Curtiss, L. A.; Weinhold, F. *Chem. Rev.* **1988**, *88*, 899.

(43) Reed, F.; Carpenter, J. E. In *The Structure of Small Molecules and Ions*; Naaman, R., Vager, Z., Eds.; Plenum Press: New York, 1988.

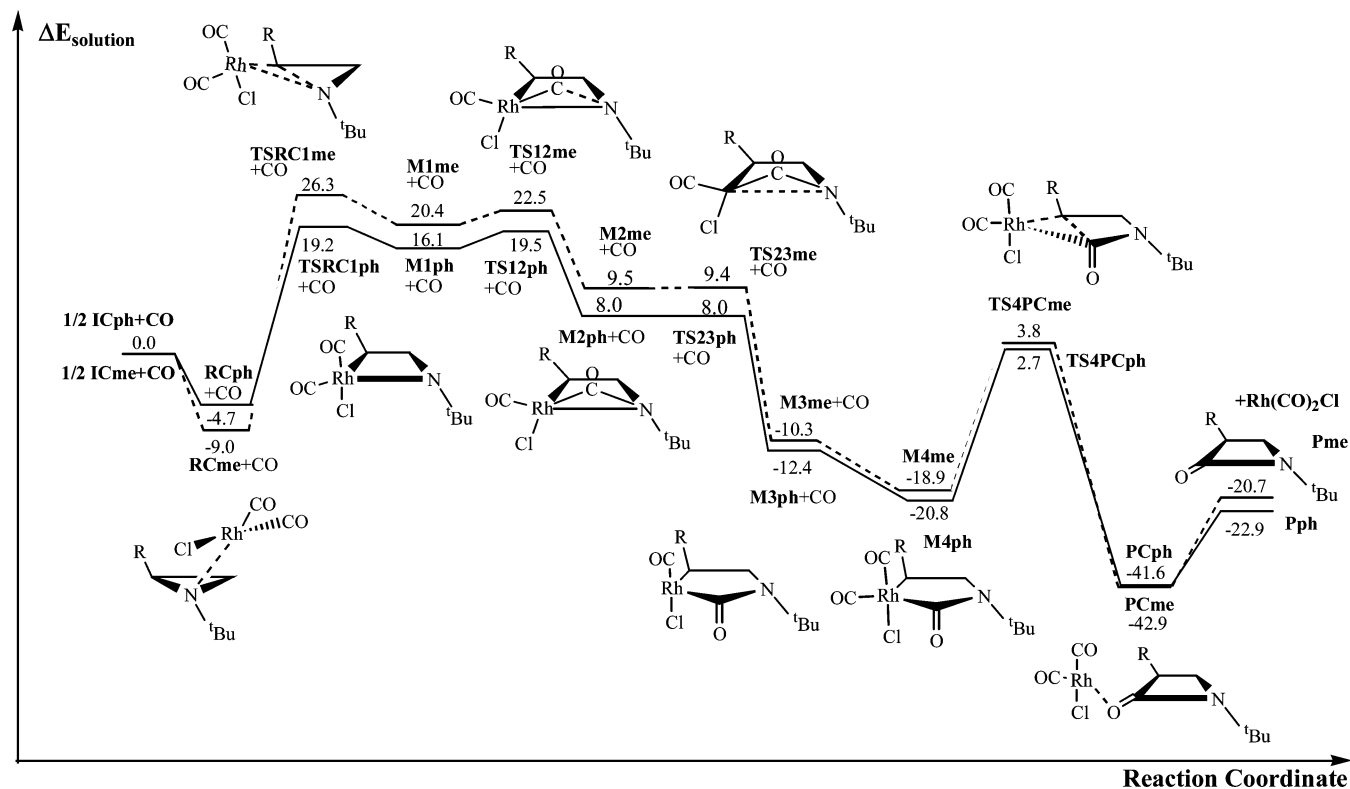


**FIGURE 1.** B3LYP/6-31G(d) (LANL2DZ for Rh) energy profiles (kcal/mol) in solution for the ring expansions of (*S*)-*N*-*tert*-butyl-2-phenylaziridine (—) and (*S*)-*N*-*tert*-butyl-2-methylaziridine (---) by insertion of the Rh(CO)<sub>2</sub>Cl monomer into the substituted C–N bond.

2-phenylaziridine. Unless otherwise stated, we will discuss in the text the relative energies in solution. As an illustration we display in Figure 3 all of the critical structures located along the insertion of Rh(CO)<sub>2</sub>Cl into the substituted C–N bond of (*S*)-*N*-*tert*-butyl-2-phenylaziridine.

#### Ring Expansion of (*S*)-*N*-*tert*-Butyl-2-phenylaziridine.

Initially the interaction between the [Rh(CO)<sub>2</sub>Cl]<sub>2</sub> dimer and two aziridine molecules gives rise to the formation of a van der Waals complex **ICph** (see Table 7S, Supporting Information). This complex dissociates<sup>44</sup> in a barrierless process to yield two monomer complexes, **RCph** (–4.7 kcal/mol),<sup>45</sup> in which the metal atom is bonded to the nitrogen atom of aziridine and presents a square planar coordination. **RCph** can evolve through the insertion of the Rh(CO)<sub>2</sub>Cl monomer into either the substituted C–N bond or the unsubstituted one.

Insertion of the Rh(CO)<sub>2</sub>Cl monomer into the substituted C–N bond gives rise to the formation of a four-membered cyclic intermediate **M1ph** (16.1 kcal/mol) through the TS, **TSRC1ph**, with an energy barrier of 23.9 kcal/mol. In **M1ph** the metal atom presents a distorted trigonal bipyramidal coordination. **M1ph** evolves through a TS, **TS12ph** (19.5 kcal/mol), for the insertion of one of the CO ligands initially coordinated to the Rh atom in the monomer into the Rh–N bond to give a bicyclic intermediate, **M2ph** (8.0 kcal/mol), in which the metal atom displays a distorted tetrahedral coordination. It must be remarked here that the insertion of an external CO molecule into the

Rh–N bond is not viable according to our computational results. Rupture of the Rh–N bond in **M2ph** yields the five-membered ring intermediate **M3ph** (–12.4 kcal/mol) in a barrierless step through **TS23ph**, which presents practically the same energy as **M2ph**.<sup>46</sup> In **M3ph** the Rh atom has a disphenoidal coordination mode. A barrierless carbonyl insertion in Rh to restore the original Rh(CO)<sub>2</sub>Cl moiety produces a new intermediate **M4ph** (–20.8 kcal/mol) in which the metal atom presents a distorted trigonal bipyramidal coordination. **M4ph** evolves through a TS, **TS4PCph**, with an energy barrier of 23.5 kcal/mol to render a complex, **PCph** (–41.6 kcal/mol), in which the metal atom is interacting with the carbonyl oxygen of the (*S*)-*N*-*tert*-butyl-3-phenyl-2-azetidinone and displays a square planar coordination. Finally, separate products (*S*)-*N*-*tert*-butyl-3-phenyl-2-azetidinone and Rh(CO)<sub>2</sub>Cl are –22.9 kcal/mol more stable than separate reactants (see Figure 1). Thus, according to our results the rate determining barrier is that corresponding to **TSRC1ph** for the insertion of the metal atom into the substituted C–N bond.

It is interesting to compare this catalytic action of the Rh monomer with that found in the catalyzed intermolecular [5 + 2] reactions between vinylcyclopropanes and alkynes where the Rh(CO)Cl is a more effective catalyst than Rh(CO)<sub>2</sub>Cl.<sup>36</sup> In the present ring expansion, however, the barrier for the attack of Rh(CO)Cl on the substituted C–N bond is about 22 kcal/mol larger than that obtained by us for the attack of Rh(CO)<sub>2</sub>Cl.

Along the ring expansion of (*S*)-*N*-*tert*-butyl-2-phenylaziridine through insertion of the Rh(CO)<sub>2</sub>Cl monomer into the unsubstituted C–N bond, the energy profile in solution is analogous

(44) Wilson, M. R.; Prock, A.; Giering, W. P.; Fernandez, A. L.; Haer, C. M.; Nolan, S. P.; Foxman, B. M. *Organometallics* **2002**, *21*, 2758.

(45) We also located a complex corresponding to the interaction of the Rh monomer with the phenyl ring 7.5 kcal/mol more stable than separate reactants in electronic energy and 2.9 kcal/mol less stable than separate reactants in solution. IRC calculations show that this complex does not belong to the reaction coordinate for the ring expansion of the aziridine.

(46) We located a TS, **TS23ph**, connecting **M2ph** with **M3ph**, which presents practically the same electronic energy as **M2ph** and becomes a transient structure when taking into account the effect of solvent.

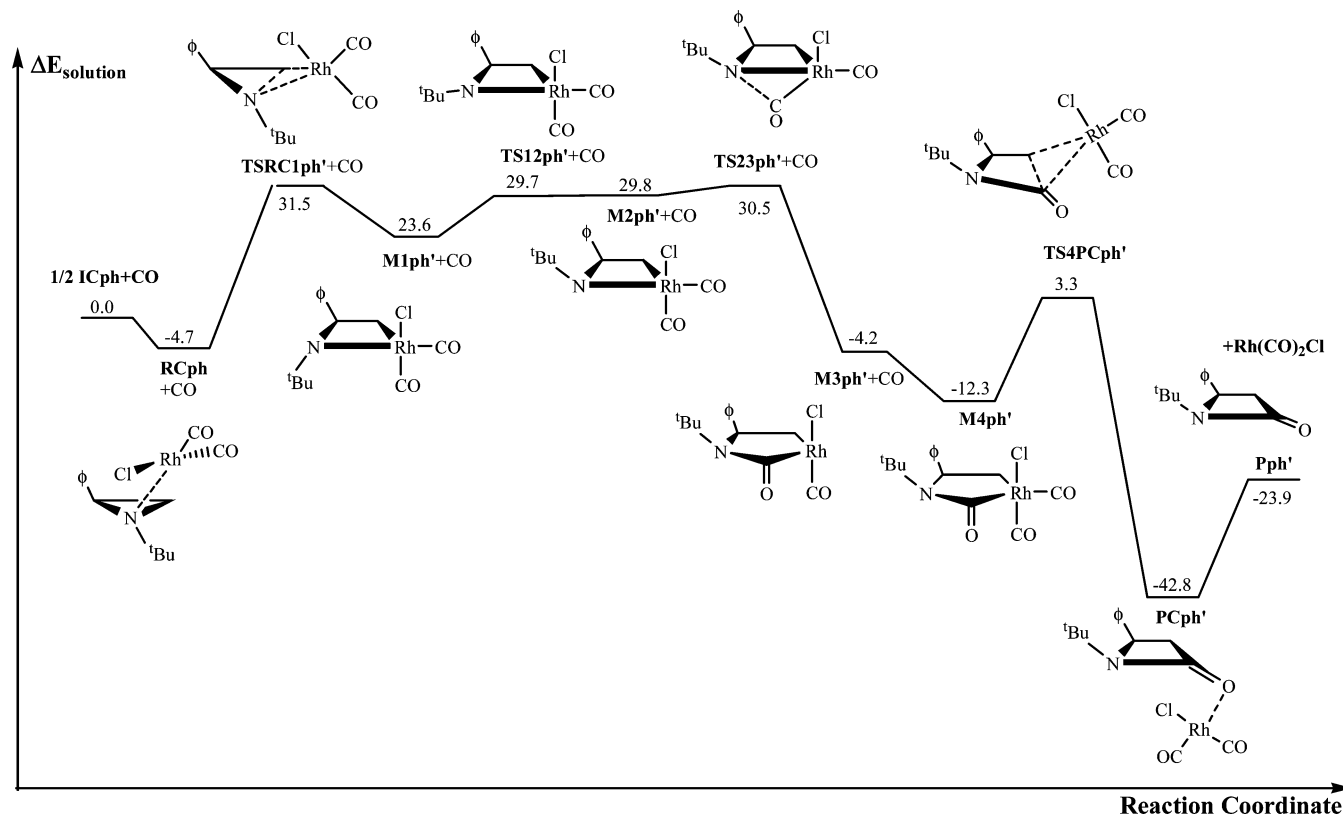


**FIGURE 2.** B3LYP/6-31G(d) (LANL2DZ for Rh) energy profile (kcal/mol) in solution for the ring expansion of (S)-N-tert-butyl-2-phenylaziridine through insertion of the  $\text{Rh}(\text{CO})_2\text{Cl}$  monomer into the unsubstituted C–N bond.

to that found for the attack on the substituted one except for the inversion of the N atom through **TS12ph'** that is now necessary for the progress of the process (see Figure 2). Now all of the critical structures located present a lower relative stability except for the product complex **PCph'**, which is 42.8 kcal/mol more stable than separate reactants (see Tables 2S and 4S in Supporting Information). As in the previous case the rate-determining TS is that for the insertion of the metal atom into the unsubstituted C–N bond, **TSRC1ph'**, although now the corresponding energy barrier is much higher (36.2 kcal/mol). Thus, our theoretical results are in agreement with the experiment that renders the (S)-N-tert-butyl-3-phenyl-2-azetidinone as the unique product.<sup>15</sup>

**Ring Expansion of (S)-N-tert-Butyl-2-methylaziridine.** In view of the results obtained for the ring expansion of (S)-N-tert-butyl-2-phenylaziridine, we only investigated the attack of  $\text{Rh}(\text{CO})_2\text{Cl}$  on the substituted C–N bond for the catalyzed ring expansion of (S)-N-tert-butyl-2-methylaziridine. In this case, the mechanism found is analogous to those for the two previous ring expansions (see Figure 1 and Tables 1S and 5S in Supporting Information). The relative stability of all of the species along the energy profile in solution is now larger than that along the ring expansion of (S)-N-tert-butyl-2-phenylaziridine to yield (S)-N-tert-butyl-3-phenyl-2-azetidinone, except for the TS **TSRC1me** for the insertion of the metal atom into the C–N bond, which presents a relative energy of 7.1 kcal/mol larger than **TSRC1ph**. **TSRC1me** is also the rate-determining TS. As, on the other hand, the relative stability of the **RCme** complex is 4.3 kcal/mol larger than that of the **RCph**, the rate-determining barrier is now 35.3 kcal/mol, 11.4 kcal/mol larger than that for the analogous ring expansion of the phenyl-substituted aziridine. This higher value of the energy barrier

would explain the experimentally observed recovery of the initial (S)-N-tert-butyl-2-methylaziridine.<sup>15</sup>

## Discussion

To investigate the origin of the regioselectivity experimentally observed<sup>12,15</sup> in the ring expansion of (S)-N-tert-butyl-2-phenylaziridine, clearly reproduced by our theoretical calculations, we analyzed the first stage of the corresponding energy profile, which includes the rate-determining TS. According to an NBO analysis the initial orientation of the phenyl ring perpendicular to the C2–C3 bond in (S)-N-tert-butyl-2-phenylaziridine (for atom numbering see Figure 4) determines the interaction between the  $\pi$  bonding C4–C5 and the  $\sigma$  antibonding C2–C3 with a second-order perturbation energy of 4.7 kcal/mol (see Figure 4). This orientation is favored by the C9–H $\cdots$ N hydrogen interaction, which presents a Mulliken overlap population of 0.022 e between H and N atoms separated 2.6 Å. The steric repulsion caused by the approach of  $\text{Rh}(\text{CO})_2\text{Cl}$  to interact with the lone pair of the nitrogen atom brings about a change in the orientation of the phenyl ring, which in the **RCph** complex is located along the C2–C3 bond. This new orientation gives rise to the interactions between the  $\pi$  bonding C4–C9 and the  $\sigma$  antibonding C3–N1 (7.5 kcal/mol) and between the  $\sigma$  bonding C3–N1 and the  $\pi$  antibonding C4–C9 (1.9 kcal/mol), thus appreciably weakening the C3–N1 bond whose bond length goes from 1.457 Å in the isolated reactant to 1.504 Å in **RCph**. Also, in this complex there is a repulsive interaction between the hydrogen atom bonded to C5 and one of the hydrogen atoms bonded to C2, which we evaluated as 4 kcal/mol approximately. These interactions then render a moderately stable complex structure in which the C3–N1 bond is signifi-

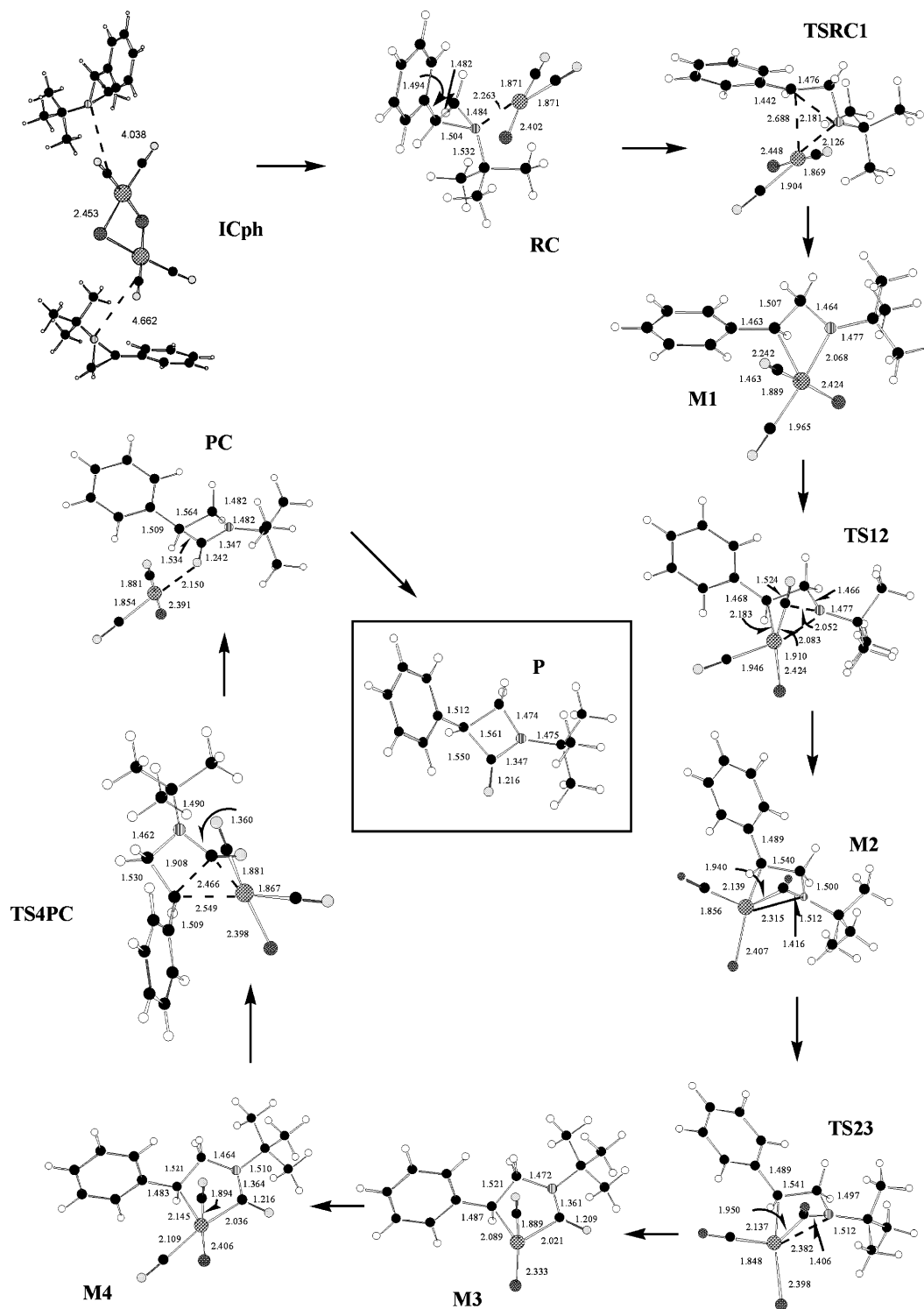


**FIGURE 3.** B3LYP/6-31G(d) optimized geometries for the structures involved in the reaction path to the ring expansion of *(S)*-*N*-*tert*-butyl-2-phenylaziridine through insertion of the  $\text{Rh}(\text{CO})_2\text{Cl}$  monomer into the substituted C–N bond. Distances are given in angstroms.

cantly activated. The activation of the C3–N1 bond crucially determines the regioselectivity of the process. According to our theoretical results this activation is triggered by the coordination of the metal atom to the nitrogen atom in the **RCph** complex. This coordination is the only mechanistic feature found by us at variance with the previous mechanistic proposal by Alper,<sup>12,15</sup> which otherwise is supported by our theoretical calculations. The position of the Rh atom in front of the C3–N1 bond in TS

**TSRC1ph** to start insertion further strengthens the interaction between this bond and the phenyl ring through the interactions between the bonding 3-center C4–C5–C6 and the antibonding C3–N1 (10.7 kcal/mol) and between the bonding C3–N1 and the antibonding C4–C5–C6 (10.8 kcal/mol) (see Figure 4). In sharp contrast with this, in the TS for the insertion of the Rh atom into the unsubstituted C2–N1 bond, **TSRC1ph'**, the only electronic rearrangement favoring the process corresponds to a

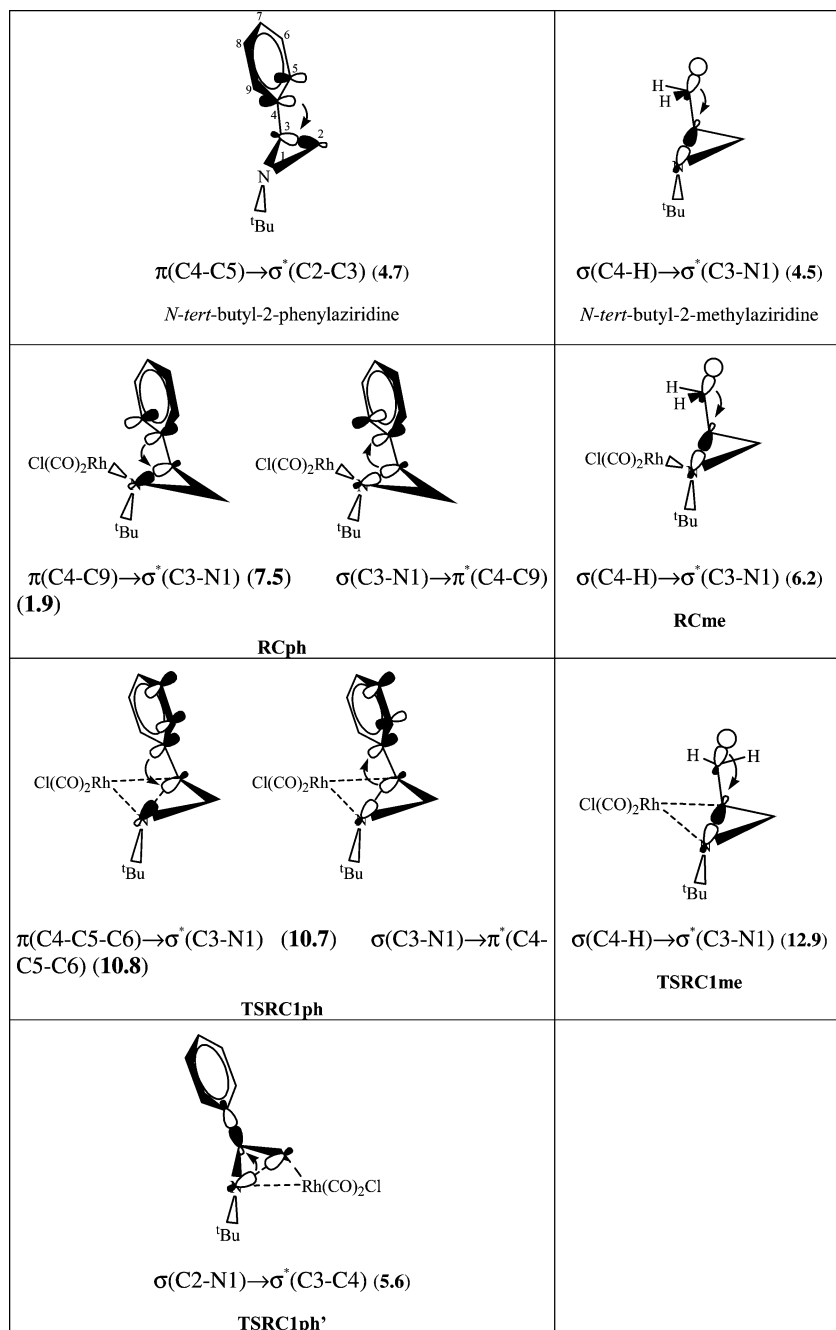


**FIGURE 4.** Most significant structures “donor-acceptor” (bond-antibond) interactions in the NBO basis for the structures involved in the first stage of the reactive processes studied. The corresponding second-order perturbation energies, in kcal/mol, are also included in parentheses.

weaker interaction between the  $\sigma$  bonding C2–N1 and the  $\sigma$  antibonding C3–C4 (5.6 kcal/mol). As a result of all of these factors, the rate-determining energy barrier for the formation of the 3-substituted  $\beta$ -lactam is the more favored one, thus explaining the regioselectivity met in the experimental work.

The present theoretical calculations also reproduce the unreactivity experimentally shown by (*S*)-*N-tert-butyl-2-methylaziridine*.<sup>15</sup> An NBO analysis shows that in **RCme** the activation of the C3–N1 bond produced by the methyl substituent is lower than that by the phenyl group in **RCph** because there is only one interaction between a bonding C–H (methyl group) and the antibonding C3–N1 (6.2 kcal/mol). On the other hand, the lack of the H $\cdots$ H repulsion present in **RCph**, the

presence of the (methyl)C–H $\cdots$ Rh (2.9 Å; Mulliken overlap population of 0.010 e) interaction, and the favorable effect of solvent (1.0 kcal/mol), make **RCme** about 4 kcal/mol more stable than **RCph** in relative energy. On the other hand, **TSRC1me** presents a relative energy 7.1 kcal/mol lower than that of **TSRC1ph**, this difference corresponding practically to the difference in the hyperconjugation interaction energies displayed in Figure 4 for these structures. These two facts would determine a considerably larger energy barrier for the ring expansion of (*S*)-*N-tert-butyl-2-methylaziridine* and explain the lack of reactivity of this molecule.

In addition, our theoretical results reproduce the enantiospecificity experimentally observed in the Rh(I)-catalyzed carbony-

lative ring expansion of  $\alpha$ -phenyl-substituted aziridines.<sup>15</sup> This is a consequence of the fact that the stereogenic center never undergoes a direct perturbation changing its configuration.

**Acknowledgment.** We are grateful to the Principado de Asturias (Spain) for financial support (PB02-045). We thank the editor and the referees for their useful comments and suggestions.

**Supporting Information Available:** Absolute electronic energies, imaginary vibrational frequencies corresponding to all transition states located along reaction paths, Cartesian coordinates corresponding to all the structures located along reaction paths, and complete Gaussian reference. This material is available free of charge via the Internet at <http://pubs.acs.org>.

JO0610356